Resonating Valence Bond Wave Functions and Classical Interacting Dimer Models

Kedar Damle, Deepak Dhar, and Kabir Ramola
Tata Institute of Fundamental Research, 1 Homi Bhabha Road, Mumbai 400005, India
(Received 20 December 2011; published 15 June 2012)

We relate properties of nearest-neighbor resonating valence-bond (NNRVB) wave functions for $SU(g)$ spin systems on two-dimensional bipartite lattices to those of fully packed interacting classical dimer models on the same lattice. The interaction energy can be expressed as a sum of n-body potentials V_n, which are recursively determined from the NNRVB wave function on finite subgraphs of the original lattice. The magnitude of the n-body interaction V_n $(n > 1)$ is of order $\mathcal{O}(g^{-(n-1)})$ for small g^{-1}. The leading term is a two-body nearest-neighbor interaction $V_2(g)$ favoring two parallel dimers on elementary plaquettes. For $SU(2)$ spins, using our calculated value of $V_2(g = 2)$, we find that the long-distance behavior of the bond-energy correlation function is dominated by an oscillatory term that decays as $1/|\vec{r}|^{\alpha}$ with $\alpha \approx 1.22$. This result is in remarkable quantitative agreement with earlier direct numerical studies of the corresponding wave function, which give $\alpha \approx 1.20$.

DOI: 10.1103/PhysRevLett.108.247216 PACS numbers: 75.10.Jm

Spin liquid states of low-dimensional insulating magnets, in which the constituent spins fail to develop any kind of long-range order down to $T = 0$ in spite of strong magnetic exchange interactions, are an interesting consequence of competing magnetic interactions in the system. Simple variational wave functions that show such behavior have played a very important role in our understanding of such states of matter [1]—the best-known examples perhaps being the resonating valence-bond (RVB) wave functions introduced by Anderson and collaborators [2,3].

The simplest of these is the nearest-neighbor RVB (NNRVB) wave function $|\Psi(g)\rangle$ for $SU(g)$ spins on a two-dimensional bipartite lattice. It is written as a uniform amplitude superposition of all possible product states in which each A-sublattice spin forms a $SU(g)$ singlet state with one of its B-sublattice neighbors [4]. Although the $g = 2$ wave function has been studied on the square lattice for over 20 years now [3], we owe a detailed understanding of its properties to much more recent work [5–7]: In Refs. [5,6], spin- and bond-energy correlations were measured in the square lattice case using Monte Carlo methods to establish that this state has an exponentially decaying spin correlation function, $|C_S(\vec{r})| \sim \exp(-|\vec{r}|/\xi)$, but power-law bond-energy correlation functions at large $|\vec{r}|$: $|C_E(\vec{r})| \sim 1/|\vec{r}|^{\alpha}$, with $\alpha \approx 1.20$. While such a short-ranged spin correlation function is a characteristic property of spin liquids, the power-law form of the bond-energy correlation functions strongly suggests that the NNRVB wave function for $SU(2)$ spins on the square lattice describes a critical state on the verge of a transition to an ordered phase in which the bond energies order.

Here, we develop a precise nonperturbative mapping that connects properties of $|\Psi(g)\rangle$ on a two-dimensional bipartite lattice to those of a classical fully packed dimer model on the same lattice, which has a nontrivial interaction potential V for the dimers in addition to the usual nonoverlapping constraint. We define a cluster expansion of V in terms of n-body potentials V_n, which are recursively determined from the NNRVB wave function on finite subgraphs of the original lattice. V_1 reduces to a constant due to the fully packed nature of the dimer model, whereas the n-body interaction V_n $(n > 1)$ is of order $\mathcal{O}(g^{-(n-1)})$ for small g^{-1} and thus decreases with n. The rate of decrease is controlled by the smallness of g^{-1}, which also controls, via this mapping, the exponential decay of spin correlation functions in $|\Psi(g)\rangle$. The most important interaction is the two-body interaction $V_2(g)$ that favors two parallel dimers on elementary plaquettes. Using our calculated value for $V_2(g = 2)$, we find that the long-distance behavior of the bond-energy correlation function in $|\Psi(g = 2)\rangle$ is dominated by an oscillatory term that decays as $1/|\vec{r}|^{\alpha}$ with

$$\alpha \approx 1.22. \tag{1}$$

Our estimate above relies on results of earlier work [8–10] on this interacting dimer model.

This result is in remarkable agreement with recent studies of the $SU(2)$ NNRVB wave function [5,6] and provides a quantitative understanding of the surprising coexistence of short-ranged spin correlations and power-law bond-energy correlations in $|\Psi(g = 2)\rangle$. Our nonperturbative mapping to an interacting fully packed classical dimer model provides a theoretical basis for the phenomenological height model description used by Tang, Sandvik, and Henley [6], which was motivated by the connection between ground states [11] of large-N $SU(N)$ antiferromagnets and fully packed dimer configurations that admit a height description [12,13].

The RVB state $|\Psi(g)\rangle$ is defined as

$$|\Psi(g)\rangle = \sum_{\mathcal{D}} |\mathcal{D}\rangle_g, \quad \text{where } |\mathcal{D}\rangle_g = \prod_{e \in \mathcal{D}} |\Phi_0(g)\rangle_e. \tag{2}$$

Here, the summation is over all fully packed dimer configurations $\mathcal{D}$, the product is over all edges e covered by a dimer in $\mathcal{D}$, and $|\Phi_0(g)\rangle_e$ is the $SU(g)$ singlet state of the two spins connected by edge e. $|\Phi_0(g)\rangle_e$ can be conveniently written in equivalent spin $S_g = (g-1)/2$ language as [14]

$$|\Phi_0(g)\rangle_e = \frac{1}{\sqrt{g}} \sum_{m=-S_g}^{S_g} (-1)^{(S_g-m)} |S^z_{e_A} = m, S^z_{e_B} = -m\rangle, \quad (3)$$

where e_A (e_B) is the A (B) sublattice site of edge e. With this natural choice of phase convention, it is easily seen that all individual terms $\langle \mathcal{D}'|\mathcal{D}\rangle_g$ are positive in the expansion for the norm

$$\langle \Psi(g)|\Psi(g)\rangle = \sum_{\mathcal{D},\mathcal{D}'} \langle \mathcal{D}'|\mathcal{D}\rangle_g. \quad (4)$$

Furthermore, since the geometric overlap of two dimer configurations $\mathcal{D}'$ and $\mathcal{D}$ gives rise to a configuration of fully packed loops (Fig. 1) in which each site belongs to exactly one nonintersecting loop, which can either be a doubled edge (consisting of a single edge traversed in both directions) or a nontrivial loop (consisting of four or more distinct edges which are each traversed once), $\langle \Psi(g)|\Psi(g)\rangle$ defines the partition function $\mathcal{Z}(g)$ of a classical fully packed loop model with positive weights $w_{\text{loop}}(g, \mathcal{L})$

$$\mathcal{Z}_{\text{loop}}(g) = \sum_{\mathcal{L}} w_{\text{loop}}(g, \mathcal{L}). \quad (5)$$

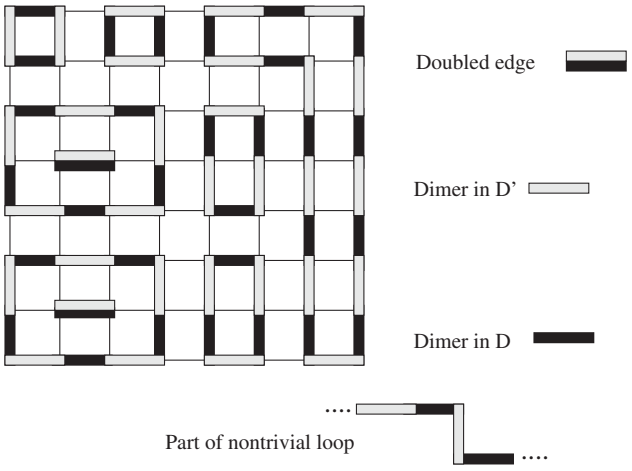

FIG. 1. $\langle \mathcal{D}'|\mathcal{D}\rangle_g$ can be represented in terms of the loop configuration $\mathcal{L}$ obtained from the overlap loops in the overlap diagram generated from dimers in $\mathcal{D}$ and $\mathcal{D}'$. Each overlap loop contributes a factor of g to $\langle \mathcal{D}'|\mathcal{D}\rangle_g$ due to the overlap of the $SU(g)$ singlet states that make up $|\mathcal{D}'\rangle_g$ and $|\mathcal{D}\rangle_g$. By convention, all overlap diagrams related by independent interchange of black and shaded dimers in each overlap loop are identified with the same loop configuration $\mathcal{L}$, and therefore $\sum_{\mathcal{D}_1,\mathcal{D}_2} \langle \mathcal{D}_2|\mathcal{D}_1\rangle_g = \sum_{\mathcal{L}} (g)^{n_d(\mathcal{L})} (2g)^{n_l(\mathcal{L})}$.

For the case of $SU(g)$ spins, one obtains [14,15]

$$w_{\text{loop}}(g, \mathcal{L}) = (g)^{n_d(\mathcal{L})} (2g)^{n_l(\mathcal{L})}, \quad (6)$$

where $n_d(\mathcal{L})$ is the number of doubled edges and $n_l(\mathcal{L})$ the number of nontrivial loops in the loop configuration $\mathcal{L}$ (Fig. 1). Expectation values of physical operators in $|\Psi(g)\rangle$ can also be related to probabilities of specific configurations of the loop gas. In the $SU(2)$ case, the spin correlation function $C_S(\vec{r}) = \langle S(0) \cdot S(\vec{r})\rangle$ is proportional to the probability that points 0 and $\vec{r}$ both lie on the same loop, while the connected bond-energy correlation function $C_{E\mu}(\vec{r}) = \langle B_\mu(0) B_\mu(\vec{r})\rangle - \langle B_\mu(0)\rangle\langle B_\mu(\vec{r})\rangle$, where $B_\mu(\vec{r}) = [\vec{S}(\vec{r}) \cdot \vec{S}(\vec{r} + \hat{\mu})]$ ($\hat{\mu} = \hat{x}, \hat{y}$ represent elementary lattice translations), is given [16] in terms of probabilities that the four points 0, $\hat{\mu}$, $\vec{r}$, and $\vec{r} + \hat{\mu}$ lie on the same loop or at most on two different loops.

Since $C_S(\vec{r})$ is proportional to the probability of points 0 and $\vec{r}$ being on the same loop, the short-range nature of C_S implies that the $g = 2$ loop model is in a "gapped" phase with predominantly short loops. Indeed, since $\mathcal{Z}_{\text{loop}}$ defines a conformally invariant loop model with a power-law distribution of loop sizes for $g = 1$ [17], we expect that this distribution becomes exponential for $g > 1$. The most natural scenario then is that the entire $g > 1$ short-loop phase of $\mathcal{Z}_{\text{loop}}$ is controlled (from a renormalization group standpoint) by the $g = \infty$ fixed point.

It is easy to see that a loop gas with extremely short loops can still have long-ranged correlations in the position and orientation of loops. More precisely, at $g = \infty$, all loops are trivial in that they have length 2, and correspond to doubled edges. We represent doubled edges by dimers to map such a loop configuration to a fully packed dimer configuration $\mathcal{D}$ on the same lattice. The weights of all such loop configurations are equal and define the partition function of a fully packed dimer model. Since all loops are doubled edges in this limit, C_S is nonzero only for nearest-neighbor spins. On the other hand, $C_{E\mu}$ maps to the connected dimer-dimer correlation function in this limit. This is known to have a power-law decay $\sim 1/|\vec{r}|^2$ on two-dimensional bipartite lattices like the square and honeycomb lattice [18,19]. Thus, at $g = \infty$, we have $|C_{E\mu}| \sim 1/|\vec{r}|^2$, although all loops are as short as they can possibly be.

For $g < \infty$, $\mathcal{Z}_{\text{loop}}$ also gets contributions from more general configurations $\mathcal{L}$ consisting of both doubled edges and nontrivial loops (with four or more edges). Each nontrivial loop in such a finite-g configuration $\mathcal{L}$ can be replaced in exactly two ways by a sequence of doubled edges on alternating edges of this nontrivial loop. Thus, a general loop configuration $\mathcal{L}$ with n_l nontrivial loops and n_d doubled edges maps to $2^{n_l(\mathcal{L})}$ different loop configurations made up purely of doubled edges, which we represent by dimers. Each finite-g configuration $\mathcal{L}$ of the original loop model thus maps to $2^{n_l(\mathcal{L})}$ dimer configurations $\mathcal{D}_\alpha$ ($\alpha = 1, 2, \ldots, 2^{n_l(\mathcal{L})}$). Next, we distribute $w_{\text{loop}}(g, \mathcal{L})$, the

original weight of $\mathcal{L}$, equally among these $\mathcal{D}_\alpha$. As a result, each of these $2^{n_l(\mathcal{L})}$ different configurations $\mathcal{D}_\alpha$ acquire an additional weight $w(g, \mathcal{L})/2^{n_l(\mathcal{L})}$. The total weight $w_{\rm dimer}(g, \mathcal{D})$ of a dimer configuration for $g < \infty$ is thus

$$w_{\rm dimer}(g, \mathcal{D}) = \sum_{\mathcal{L}|\mathcal{D}} \frac{w_{\rm loop}(g, \mathcal{L})}{2^{n_l(\mathcal{L})}}, \tag{7}$$

where $\mathcal{L}|\mathcal{D}$ denotes all loop configurations $\mathcal{L}$ obtained from the overlap of $\mathcal{D}$ with any other fully packed dimer configuration $\mathcal{D}'$.

Equivalently, we may define $w_{\rm dimer}(g, \mathcal{D})$ via

$$w_{\rm dimer}(g, \mathcal{D}) = \langle \mathbf{\Psi}(g)|\mathcal{D}\rangle_g. \tag{8}$$

The original loop partition function $\mathcal{Z}_{\rm loop}$ is then equal to the partition sum over all fully packed dimer configurations $\mathcal{D}$ with weights $w_{\rm dimer}(g, \mathcal{D})$:

$$\mathcal{Z}_{\rm loop} = \mathcal{Z}_{\rm dimer} = \sum_{\mathcal{D}} w_{\rm dimer}(g, \mathcal{D}). \tag{9}$$

The energy $V(g, \mathcal{D})$ of a dimer configuration $\mathcal{D}$ in this classical interacting fully packed dimer model is defined as

$$V(g, \mathcal{D}) = -\log[w_{\rm dimer}(g, \mathcal{D})]. \tag{10}$$

We now define a decomposition of the energy $V(g, \mathcal{D})$ into a sum of n-body potential energies $V_n(\mathcal{D}_n)$ of subconfigurations $\mathcal{D}_n$ consisting of n distinct dimers from $\mathcal{D}$,

$$V(g, \mathcal{D}) = \sum_n \sum_{\mathcal{D}_n \in \mathcal{D}} V_n(\mathcal{D}_n). \tag{11}$$

The V_n are determined recursively from computation of the weight $w^{\mathcal{G}_n}_{\rm dimer}(g, \mathcal{D}_n)$ of $\mathcal{D}_n$ in the interacting dimer model on the finite subgraph $\mathcal{G}_n(\mathcal{D}_n)$ of the square lattice. Here, this weight is calculated via Eq. (7) from the loop model defined on $\mathcal{G}_n(\mathcal{D}_n)$, and the subgraph $\mathcal{G}_n(\mathcal{D}_n)$ consists of the $2n$ vertices covered by dimers of the subconfiguration $\mathcal{D}_n$, along with all allowed edges between these vertices.

In the first step of this recursive construction, we consider any particular $\mathcal{D}_1$ and determine the weight $w^{\mathcal{G}_1}_{\rm dimer}(g, \mathcal{D}_1)$. The original loop model on $\mathcal{G}_1(\mathcal{D}_1)$ has only one valid configuration, which is a doubled edge on the only edge of $\mathcal{G}_1(\mathcal{D}_1)$. Using Eq. (7), we therefore have $w^{\mathcal{G}_1}_{\rm dimer}(g, \mathcal{D}_1) = g$. The logarithm of this weight defines the one-body potential

$$V_1(\text{▬}) = V_1(\text{▮}) = -\log(g)\ . \tag{12}$$

With this in hand, V_n for arbitrary n can be obtained recursively from the equation

$$-\log[w^{\mathcal{G}_n}_{\rm dimer}(g, \mathcal{D}_n)] = V_n(\mathcal{D}_n) + \sum_{m=1}^{n-1} \sum_{\mathcal{D}_m \in \mathcal{D}_n} V_m(\mathcal{D}_m), \tag{13}$$

where $\mathcal{D}_m \in \mathcal{D}_n$ denotes all m-dimer subconfigurations $\mathcal{D}_m$ of $\mathcal{D}_n$, and $\mathcal{G}_m(\mathcal{D}_m)$ denotes the corresponding subgraphs of $\mathcal{G}_n(\mathcal{D}_n)$.

For instance, to obtain V_2, we consider any particular $\mathcal{D}_2$ and determine $w^{\mathcal{G}_2}_{\rm dimer}(\mathcal{D}_2)$ as follows: If $\mathcal{G}_2(\mathcal{D}_2)$ does not form a plaquette of the square lattice, there is only one valid configuration of the loop model on $\mathcal{G}_2(\mathcal{D}_2)$ and Eq. (7) gives $w^{\mathcal{G}_2}_{\rm dimer}(\mathcal{D}_2) = g^2$. On the other hand, when $\mathcal{G}_2(\mathcal{D}_2)$ does form a plaquette of the square lattice, $w^{\mathcal{G}_2}_{\rm dimer}(\mathcal{D}_2)$ gets contributions from two of the three valid configurations of the loop model on $\mathcal{G}_2(\mathcal{D}_2)$, and Eqn. (7) gives $w^{\mathcal{G}_2}_{\rm dimer}(\mathcal{D}_2) = g^2 + g$. Knowing $w^{\mathcal{G}_2}_{\rm dimer}(\mathcal{D}_2)$, V_2 can be obtained from the recursion relation Eq. (13) with $n = 2$. Clearly, V_2 is nonzero only if the two dimers live on the same plaquette of the square lattice, and in this nontrivial case we obtain

$$V_2(\text{⊟}) = V_2(\text{◫}) = -\log(1 + g^{-1})\ . \tag{14}$$

Similarly, V_3 is seen to be zero unless the three dimers live on a pair of adjacent plaquettes, and in this nontrivial case we obtain

$$V_3(\text{⊟⊐}) = -\log\left[(1 + g^{-1} + g^{-2})(1 + g^{-1})^{-1}\right]\ ,$$
$$V_3(\text{◫▮}) = -\log\left[(1 + 2g^{-1})(1 + g^{-1})^{-2}\right]\ , \tag{15}$$

and the symmetry-related counterparts of Eq. (15) obtained by using lattice reflection and rotation symmetries.

It is clear that each V_n for $n > 1$ is of order $\mathcal{O}(g^{-(n-1)})$ when the n dimers live on a contiguous set of plaquettes of the square lattice (sharing edges with each other) and zero otherwise. Our procedure thus expands V in the size of clusters and is controlled by the smallness of g^{-1}. It may be viewed as a classical version of the "Schrieffer-Wolff"canonical transformation approach familiar in the context of strongly interacting electronic systems; in the usual [20] Schrieffer-Wolff transformation, the effects of higher-energy states in a larger Hilbert space are encoded in modifications to the effective Hamiltonian that acts in the subspace of low-energy states, whereas in our classical version of this approach, loop model configurations containing nontrivial loops are accounted for by effective weights $w_{\rm dimer}(g, \mathcal{D})$ of dimer configurations $\mathcal{D}$.

To calculate expectation values $\langle \mathbf{\Psi}(g)|\hat{O}|\mathbf{\Psi}(g)\rangle$ in dimer language, we construct a modified estimator $\bar{\mathcal{P}}_{\hat{O}}(\mathcal{D})$ that correctly encodes the contributions from all loop model configurations, including those with nontrivial loops

$$\bar{\mathcal{P}}_{\hat{O}}(\mathcal{D}) = \frac{1}{w_{\rm dimer}(g, \mathcal{D})} \sum_{\mathcal{L}|\mathcal{D}} \frac{w_{\rm loop}(g, \mathcal{L}) \mathcal{P}_{\hat{O}}(\mathcal{L})}{2^{n_l(\mathcal{L})}}, \tag{16}$$

where $\mathcal{P}_{\hat{O}}(\mathcal{L})$ denotes the contribution of $\mathcal{L}$ to $\langle \mathbf{\Psi}(g)|\hat{O}|\mathbf{\Psi}(g)\rangle$ in loop-gas language [14,16].

Consider for instance the spin correlation function. To zeroth order in g^{-1}, the corresponding modified estimator is nonzero only if 0 and $\vec{r}$ are connected by a dimer in $\mathcal{D}$, while the $\mathcal{O}(g^{-1})$ correction gives an additional contribution if 0 and $\vec{r}$ belong to the same flippable plaquette of $\mathcal{D}$,

and so on. In the case of the bond-energy correlation function $C_{E_\mu}(\vec{r})$, we see that the large $|\vec{r}|$ behavior is dominated by the first $\mathcal{O}(g^0)$ term, which is obtained by replacing each $B_\mu(\vec{r})$ by the dimer occupation number $n_\mu(\vec{r})$ of the corresponding edge in the dimer model

$$C_{E_\mu}(\vec{r}) \sim \langle n_\mu(0) n_\mu(\vec{r})\rangle_V - \langle n_\mu(0)\rangle_V \langle n_\mu(\vec{r})\rangle_V, \qquad (17)$$

where $\langle \ldots \rangle_V$ denotes averages computed in the dimer model with energy V.

As is well-known, such fully packed dimer models (with or without interactions) admit a microscopic height representation [9,10,12,13], which upon coarse graining leads to a coarse-grained height action that takes the form

$$S = \pi\rho \int d^2 r (\nabla h)^2 + \sum_{p=4,8,12\ldots} y_p \int d^2 r \cos(2\pi p h) + \cdots, \qquad (18)$$

where the ellipses denote higher gradient terms and higher powers of gradients consistent with symmetries [12] and the bare coefficients ρ and y_p are functions of g. The renormalization group theory for this height action is standard [12,21]: In the present variables, it tells us that there is a line of fixed points $\rho^* = \kappa$, $y_p^* = 0$ with $0 < \kappa \leq 4$. As long as the bare values of ρ, y_p, and the coefficients of the omitted higher derivative and nonlinear terms are not too large, the system flows to an attractive fixed point $\kappa(g)$ on this fixed line.

As mentioned earlier, the $g \to \infty$ limit maps to a noninteracting dimer model since all interactions (V_n with $n > 1$) vanish and V_1 simply represents the fugacity g of each dimer. Therefore, we expect $\kappa(g \to \infty) = 1/2$ since this is the known value of the stiffness for a noninteracting dimer model on the square lattice [12]. As g is reduced from $g = \infty$, the leading effect is an interaction V_2 that favors flippable plaquettes. The interacting dimer model with only V_2 present has been studied in detail in Refs. [8–10], which established that the renormalized stiffness κ increases monotonically with the magnitude of V_2 until it reaches $\kappa = 4$, at which point the system undergoes a Kosterlitz-Thouless-like transition to a columnar ordered state.

To access the qualitative behavior of correlations in the NNRVB wave function of $SU(2)$ spins, we note that the magnitude of V_2 is precisely equal to the inverse temperature parameter β of Ref. [9]. Setting $g = 2$, we therefore have $\beta = \log(1 + g^{-1}) \approx 0.405$ [22]. This places us deep in the high-temperature phase well above the transition to columnar order, and from Fig. 31 of Ref. [9], we obtain the estimate $\kappa(g = 2) \approx 0.82$. Calculating the required dimer correlation function from the fixed-point height action with this value of κ using the standard correspondence between dimer occupation numbers and the height field [12,13], we obtain the leading, large $|\vec{r}|$ form of the bond-energy correlation functions

$$C_{E_x}(\vec{r}) \sim \frac{(-1)^x}{|\vec{r}|^{1/\kappa(g)}}; \qquad C_{E_y}(\vec{r}) \sim \frac{(-1)^y}{|\vec{r}|^{1/\kappa(g)}}, \qquad (19)$$

which gives, upon setting $g = 2$, the leading order estimate advertised earlier. In addition, both these correlation functions have a subdominant piece which goes as $(-1)^{x+y}/|\vec{r}|^2$ independent of $\kappa(g)$.

What about subleading (higher order in g^{-1}) corrections to this leading order result? Note that higher-order corrections arise from two sources—one is the modified estimator mentioned earlier and the other is the effect of three-body and higher interaction terms in the interacting dimer model. It is easy to see that modifications to the estimator will affect the prefactor but not the leading power-law behavior of the energy correlators at long distances. On the other hand, inclusion of three-body and higher interactions will change the stiffness κ of the interacting dimer model and thus the exponent κ^{-1} of the power-law decay. In the Supplemental Material [24], we argue that these higher-order effects come in with alternating signs in the expansion for κ^{-1} as a function of g^{-1}. This is because the leading two-body interaction favors columnar order of dimers and drives κ to higher values, whereas the subleading three-body interaction disfavors columnar order, leading to a slight reduction in κ, and so on.

We conclude by noting that our approach generalizes in an obvious way to include singlets between A- and B-sublattice sites that are further apart on the square lattice, as well as to the $SU(g)$ NNRVB wave function on the honeycomb lattice. Again, we expect the corresponding loop models to be in a short-loop phase for all $g > 1$, and this allows us to access the properties of these wave functions for $g \geq 2$ by a mapping to an interacting dimer model; on the honeycomb lattice, the leading interaction terms will favor flippable hexagons, whereas the presence of longer-range singlets in the square lattice case will introduce additional interactions. Possible generalizations to various three-dimensional bipartite lattices are more intriguing, especially since the NNRVB wave function for $SU(2)$ spins appears to possess long-range antiferromagnetic spin order coexisting with power-law bond-energy correlators in some cases, perhaps necessitating a different approach for its description [25].

We acknowledge the computational resources of TIFR and research support from the Indo-French Centre for the Promotion of Advanced Research (IFCPAR/CEFIPRA) under Project 4504-1 (K. D.) and from the Indian DST via Grants No. DST-SR/S2/RJN-25/2006 (K. D.) and No. DST-SR/S2/JCB-24/2005 (D. D.). We thank F. Alet for a critical reading of an earlier draft of this manuscript. One of us (K. D.) would also like to thank the organizers and all participants of the Toulouse Workshop on Quantum Magnetism, particularly F. Alet, R. Moessner, and A. Sandvik, for interesting and insightful discussions and ICTS-TIFR and IISc Bangalore for hospitality during completion of this work.

[1] X. G. Wen, *Quantum Field Theory of Many-Body Systems* (Oxford University, New York, 2004).
[2] P. Fazekas and P. W. Anderson, Philos. Mag. **30**, 423 (1974).
[3] S. Liang, B. Doucot, and P. W. Anderson, Phys. Rev. Lett. **61**, 365 (1988).
[4] Spins on the A sublattice carry the fundamental representation of $SU(g)$, whereas those on the B sublattice carry the complex conjugate of this.
[5] A. F. Albuquerque and F. Alet, Phys. Rev. B **82**, 180408 (R) (2010).
[6] Y. Tang, A. W. Sandvik, and C. L. Henley, Phys. Rev. B **84**, 174427 (2011).
[7] J. Cano and P. Fendley, Phys. Rev. Lett. **105**, 067205 (2010).
[8] F. Alet, J. L. Jacobsen, G. Misguich, V. Pasquier, F. Mila, and M. Troyer, Phys. Rev. Lett. **94**, 235702 (2005).
[9] F. Alet, Y. Ikhlef, J. L. Jacobsen, G. Misguich, and V. Pasquier, Phys. Rev. E **74**, 041124 (2006).
[10] S. Papanikolaou, E. Luijten, and E. Fradkin, Phys. Rev. B **76**, 134514 (2007).
[11] N. Read and S. Sachdev, Phys. Rev. B **42**, 4568 (1990).
[12] E. Fradkin, D. A. Huse, R. Moessner, V. Oganesyan, and S. L. Sondhi, Phys. Rev. B **69**, 224415 (2004).
[13] C. L. Henley, J. Phys. Condens. Matter **16**, S891 (2004).
[14] K. S. D. Beach, F. Alet, M. Mambrini, and S. Capponi, Phys. Rev. B **80**, 184401 (2009).
[15] J. Lou, A. W. Sandvik, and N. Kawashima, Phys. Rev. B **80**, 180414 (2009).
[16] K. S. D. Beach and A. W. Sandvik, Nucl. Phys. **B750**, 142 (2006).
[17] R. Kenyon, arXiv:1105.4158.
[18] M. E. Fisher and J. Stephenson, Phys. Rev. **132**, 1411 (1963).
[19] R. Youngblood, J. D. Axe, and B. M. McCoy, Phys. Rev. B **21**, 5212 (1980).
[20] J. R. Schrieffer and P. A. Wolff, Phys. Rev. **149**, 491 (1966).
[21] J. V. Jose, L. P. Kadanoff, S. Kirkpatrick, and D. R. Nelson, Phys. Rev. B **16**, 1217 (1977).
[22] It may be possible to improve this estimate of β by partial resummation of the effects of three-body and higher couplings, along the lines of the analysis in Ref. [23].
[23] D. Schwandt, M. Mambrini, and D. Poilblanc, Phys. Rev. B **81**, 214413 (2010).
[24] See Supplemental Material at http://link.aps.org/supplemental/10.1103/PhysRevLett.108.247216 for a discussion of higher order effects.
[25] A. F. Albuquerque, F. Alet, and R. Moessner, arXiv:1204.3195.